



Investigating the physiological ecology of mesopelagic zooplankton in the Scotia sea (Southern ocean) using lipid and stable isotope signatures

Eloïse Linda-Roselyne Savineau^{a,b,*}, Kathryn B. Cook^{b,c}, Sabena J. Blackbird^d, Gabriele Stowasser^e, Konstadinos Kiriakoulakis^f, Calum Preece^d, Sophie Fielding^e, Anna C. Belcher^e, George A. Wolff^d, Geraint A. Tarling^e, Daniel J. Mayor^{b,c}

^a School of Ocean and Earth Science, University of Southampton, Southampton, SO14 3ZH, UK

^b National Oceanography Centre, Southampton, SO14 3ZH, UK

^c Biosciences, Hatherly Building, University of Exeter, Exeter, EX4 4 PS, UK

^d School of Environmental Sciences, University of Liverpool, Liverpool, L69 3GP, UK

^e British Antarctic Survey, Cambridge, CB3 0ET, UK

^f School of Biological and Environmental Sciences, Liverpool John Moores University, Liverpool, L3 3AF, UK

ARTICLE INFO

Keywords:

Copepods
Amphipods
Euphausiids
Salps
Chaetognatha
Trophic interactions
Fatty acids
South Georgia
Twilight zone

ABSTRACT

The mesopelagic zooplankton community plays an important role in the cycling and sequestration of carbon via the biological pump. However, little is known about the physiology and ecology of key taxa found within this region, hindering our understanding of their influence on the pathways of energy and organic matter cycling. We sampled the eight most abundant zooplankton (*Calanoides acutus*, *Rhincalanus gigas*, *Paraeuchaeta* spp., Chaetognatha, *Euphausia triacantha*, *Thysanoessa* spp., *Themisto gaudichaudii* and *Salpa thompsoni*) from within the mesopelagic zone in the Scotia Sea during a sinking diatom bloom and investigated their physiological ecology using lipid biomarkers and stable isotopic signatures of nitrogen. Data suggest that the large calanoid copepods, *C. acutus* and *R. gigas*, were in, or emerging from, a period of metabolic inactivity during the study period (November 15th – December 15th 2017). Abundant, but decreasing lipid reserves in the predominantly herbivorous calanoid copepods, suggest these animals may have been metabolising previously stored lipids at the time of sampling, rather than deriving energy solely from the diatom bloom. This highlights the importance of understanding the timing of diapause of overwintering species as their feeding is likely to have an impact on the turnover of particulate organic matter (POM) in the upper mesopelagic. The $\delta^{15}\text{N}$ signatures of POM became enriched with increasing depth, whereas all species of zooplankton except *T. gaudichaudii* did not. This suggests that animals were feeding on fresher, surface-derived POM, rather than reworked particles at depth, likely influencing the quantity and quality of organic matter leaving the upper mesopelagic. Our study highlights the complexity of mesopelagic food webs and suggests that the application of broad trophic functional types may lead to an incorrect understanding of ecosystem dynamics.

1. Introduction

The biological carbon pump (BCP) refers to the myriad processes that export photosynthetically-fixed particulate organic matter (POM) from the ocean's surface into deeper waters (Boyd et al., 2019) where it may subsequently be stored for tens or hundreds of years, depending on the depth of remineralisation (Kwon et al., 2009). Zooplankton are known to influence the strength of the BCP through numerous processes, including grazing on phytoplankton, repackaging POM into faecal

pellets, active transport of carbon by diel and ontogenetic vertical migration, and fragmentation of sinking particles (Turner, 2015; Steinberg and Landry, 2017; Mayor et al., 2020; Anderson et al., 2022).

Zooplankton in the mesopelagic zone, between ~100 and 1000 m, act as a trophic filter between surface productivity and the deep ocean (Giering et al., 2014; Mayor et al., 2014, 2020). However, relatively little is known about the physiology and trophic interactions of these animals, hindering our understanding of the pathways of energy and organic matter processing in this environment. Zooplankton obtain their

* Corresponding author. School of Ocean and Earth Science, University of Southampton, Southampton, SO14 3ZH, UK.

E-mail address: eloise.savineau@soton.ac.uk (E.L.-R. Savineau).

<https://doi.org/10.1016/j.dsr.2024.104317>

Received 16 January 2024; Received in revised form 24 April 2024; Accepted 2 May 2024

Available online 7 May 2024

0967-0637/© 2024 The Authors. Published by Elsevier Ltd. This is an open access article under the CC BY license (<http://creativecommons.org/licenses/by/4.0/>).

food in several ways, including feeding on phytoplankton, consuming detritus/sinking particles, or carnivory. Moreover, trophic interactions are rarely “black and white”, with zooplankton showing feeding plasticity due to both spatial and temporal variability in food availability (Søreide et al., 2008; de Moura et al., 2016).

Stable isotope ratios of nitrogen ($\delta^{15}\text{N}$) are commonly used to estimate trophic position as the heavier isotope, ^{15}N , is retained and accumulated in the tissues of organisms preferentially over the lighter isotope, ^{14}N , with increasing trophic level (Miyake and Wada, 1967). Stable isotope analysis allows for the calculation of trophic levels within a food web but does not provide information on the specificity of a consumer's diet and is therefore often conducted in parallel with other complementary techniques, such as lipid biomarkers (Protopapa et al., 2019). Lipid biomarkers have widely been used as a tool to investigate the feeding ecology and physiology of zooplankton (Dalsgaard et al., 2003; Wilson et al., 2010; Pond et al., 2012; Stevens et al., 2022). Fatty acids can be obtained either through the consumer's diet or *de novo* biosynthesis. Bacteria, algae and some zooplankton biosynthesize specific fatty acids, which can then be transferred through the food web and accumulated in lipids of consumers, sometimes without modification, making them useful trophic biomarkers. Many species of calanoid copepods biosynthesize the fatty acids 20:1(n-9) and 22:1(n-11), which are referred to as calanoid biomarkers (Hagen et al., 1993; Kattner and Hagen, 1995). These fatty acids, and their fatty alcohol counterparts, are prominent moieties in the wax esters that many calanoid copepods use to store energy (Hagen et al., 1993; Lee et al., 2006). Two polyunsaturated fatty acids (PUFAs), 20:5(n-3) and 22:6(n-3) (commonly known as EPA and DHA, respectively), are predominantly biosynthesized *de novo* by diatoms and dinoflagellates, respectively, and are considered valuable biomarkers for sources of herbivory as they cannot be biosynthesized by zooplankton at biologically significant rates (Bell et al., 2007). Lipids can give insight into key physiological processes of zooplankton, such as energetic and physiological adaptation of diapausing species (Visser and Jónasdóttir, 1999; Pond, 2012). Vertically migrating zooplankton increase the proportion of 22:6(n-3) in their phospholipids in response to increasing pressure and decreasing temperature throughout the epi- to mesopelagic (Pond et al., 2014). Fatty acid signatures are therefore not simply biomarkers of diet, but rather a reflection of metabolic processes that store, synthesize, and catabolise lipids to meet physiological requirements (Mayor et al., 2011, 2013).

The Scotia Sea is considered to be one of the most productive areas of the Southwest Atlantic/Southern Ocean, with large phytoplankton blooms dominated by diatoms (Korb et al., 2012) and high zooplankton biomass (Atkinson et al., 2004; Ward et al., 2012). Here, we explore the trophic- and physiological ecology of zooplankton from within the mesopelagic region of the Scotia Sea using $\delta^{15}\text{N}$ and lipid signatures in the eight most abundant and biomass-dominant taxa. We integrate these data and use them to examine how different diet- and life-history-related physiologies influence the observed patterns in biomarkers in the different animals sampled. We moreover compare zooplankton lipid and stable isotope signatures to those of POM (see also Preece et al., Submitted), to determine the fate of POM within the food web during a spring bloom and hence how zooplankton influence the cycling of POM within the epi- and upper mesopelagic.

2. Methods

2.1. Sample collection

This study is part of the COMICS (Controls over Ocean Mesopelagic Interior Carbon Storage) programme, which aims to shed light on the processes controlling carbon remineralisation in the mesopelagic (Sanders et al., 2016). Samples were collected aboard the *RRS Discovery* during the research cruise DY086 to the Scotia Sea in the Southern Ocean (12 November – December 19, 2017) in the vicinity of the British Antarctic Survey Scotia Sea open-ocean observatory site P3 (SCOOBIES,

52.40 S, 40.06 W) (Giering et al., 2019). The same station was visited 3 times, defined as P3A (15–22nd November), P3B (29th November – 5th December) and P3C (9–15th December).

Samples for stable isotope analyses of POM were collected in Niskin bottles via a CTD rosette deployed at depths approximately corresponding to the sampled net horizon depths (5, 25, 50, 75, 125, 200, 450 m). Samples were filtered onto pre-combusted (450 °C; 12 h) 47 mm GF/F filters (Whatman glass fibre filter, nominal pore size 0.7 μm) and stored frozen at $-80\text{ }^\circ\text{C}$ prior to analysis. Samples for lipid analyses of POM were obtained using standalone pumps (SAPs) deployed within the mixed layer (ML; 0–90 m), the upper mesopelagic, 150–170 m (i.e. ca. ML + 100 m), 250–260 m (ca. ML + 200 m), and 440–460 m. Two size fractions were sampled. Large particles ($>53\text{ }\mu\text{m}$) were collected on nylon mesh screens (Nitex; pore size 53 μm ; 10 % HCl acid cleaned). Small particles (0.7–53 μm , $<53\text{ }\mu\text{m}$ hereafter) were collected on pre-combusted (400 °C; 4 h) 293 mm GF/F filters (nominal pore size 0.7 μm) located under the nylon mesh (Full SAPs filtration protocol can be found in Preece et al., Submitted). All visible zooplankton/organisms were removed from the filters.

A range of nets were used to capture the vertical distribution of the epipelagic and upper mesopelagic (0–500 m) mesozooplankton, macrozooplankton and micronekton $>0.3\text{ mm}$. Animals were collected with a combination of RMT 25 (Rectangular Midwater Trawl, 25 m^2 net mouth, 4 mm cod-end mesh), MOCNESS (Multiple Opening and Closing Net and Environmental Sampling System, 1 m^2 rectangular opening, 330 μm (0.33 mm) mesh nets) and Mammoth Net (300 μm mesh, 1 m^2 opening) (see Supplementary Tables S1 and S2). The nets were deployed over a range of discrete depth intervals from 500 m to the surface, deployed either obliquely (RMT25 and MOCNESS), or vertically (MAMMOTH). Full net deployment protocols can be found in Cook et al. (2023). Once onboard, the net cod ends were immediately transferred into a temperature-controlled laboratory (2 °C) and specimens of the eight most abundant zooplankton taxa were subsequently picked: *Calanoides acutus*, *Rhincalanus gigas* and *Paraeuchaeta* spp. (Calanoida); Chaetognatha; *Euphausia triacantha* and *Thysanoessa* spp. (Euphausiacea); *Themisto gaudichaudii* (Amphipoda); and *Salpa thompsoni* (Salpida). Chaetognaths were not identified to species level. Insufficient *T. gaudichaudii* were collected at depths beyond 250 m for analysis. Samples for stable isotope and lipid analyses were stored in petri dishes and glass vials, respectively and frozen at $-80\text{ }^\circ\text{C}$.

2.2. Stable isotope analyses

Invertebrate specimens were weighed (wet weight), freeze-dried whole and then re-weighed (dry weight). Samples were homogenised using an oscillating mill (MM200, Retsch). Isotopic analyses were carried out at the Scottish Universities Research Centre (SUERC), East Kilbride, Glasgow, UK. Aliquots for nitrogen isotopes were weighed into tin capsules (0.6 – 1 mg) and measured on a Thermo-Fisher-Scientific (Bremen, Germany) Delta XP Plus Isotope-Ratio Mass Spectrometer linked to an Elementar (Hanau, Germany) Pyrocube Elemental Analyser. The internal reference materials were GEL (gelatin solution, $\delta^{15}\text{N} = 5.71 \pm 0.15\text{‰}$), ALAGEL (alanine-gelatine solution, $\delta^{15}\text{N} = 2.52 \pm 0.08\text{‰}$), and GLYGEL (glycine-gelatine solution spiked with ^{15}N -alanine, $\delta^{15}\text{N} = 23.60 \pm 0.12\text{‰}$), each dried for 2 h at 70 °C. Four USGS40 glutamic acid standards 106, 107 were used as independent checks of precision and accuracy. Delta values were corrected for instrument drift and linearity. Delta (δ) values are used to express the relative difference between the ratios of two stable isotopes, ^{15}N and ^{14}N in organisms, expressed as $\delta^{15}\text{N}$, compared to the international reference standard for nitrogen isotopes ($\delta^{15}\text{N}$ of atmospheric nitrogen gas).

Trophic level (TL) was calculated from $\delta^{15}\text{N}$ following the equation:

$$TL = \frac{(\delta^{15}\text{N}_{\text{consumer}} - \delta^{15}\text{N}_{\text{primary consumer}})}{\Delta_n} + 2.0$$

where $\delta^{15}\text{N}_{\text{consumer}}$ is the $\delta^{15}\text{N}$ signature of the consumer of interest, $\delta^{15}\text{N}_{\text{primary consumer}}$ is the $\delta^{15}\text{N}$ of a primary consumer, here assumed to be the herbivorous copepod *C. acutus*, 2.0 is the trophic level of the primary consumer (Post, 2002), Δ_n is the $\delta^{15}\text{N}$ enrichment factor per trophic level (2.5 ‰ for herbivores; (Vander Zanden and Rasmussen, 2001). Using $\delta^{15}\text{N}$ of a primary consumer allows for reduced susceptibility of short-term phytoplankton seasonal changes influencing baseline isotopic signatures (Cabana and Rasmussen, 1996). The use of a herbivorous calanoid copepod as the baseline consumer has been suggested as a more appropriate method in high-chlorophyll α conditions dominated by diatoms, which often pass through other primary consumers, such as salps, undigested (von Harbou et al., 2011; Metfies et al., 2014; Pakhomov et al., 2019).

2.3. Lipid analysis

Zooplankton lipid extractions were carried out on each homogenised freeze-dried ($-60\text{ }^\circ\text{C}$; 10^{-2} mBar) sample (1–60 mg dry weight) (Cook et al., 2023). A known quantity of an internal standard (3–10 μg L of 5 α (H)-cholestane) was added to each sample, followed by a mixture of dichloromethane (DCM) and methanol (9:1; 15 mL). The samples were then sonicated (15 min, x2) and the resulting extract was decanted into round bottom flasks. The solvent obtained was evaporated to dryness under vacuum using a rotary evaporator at $\sim 30\text{ }^\circ\text{C}$. Each sample was then passed through a Pasteur pipette filled with anhydrous sodium sulphate using DCM (3 mL). The solvent was blown down with nitrogen gas and the samples were stored ($-20\text{ }^\circ\text{C}$) before transmethylation and derivatisation with N,O-bis-(trimethylsilyl)trifluoroacetamide (BSTFA). Lipids from the POM samples were extracted in a similar way (see also Kiriakoulakis et al., 2004).

Gas chromatography-mass spectrometry (GC-MS) analyses of the total lipid extracts were conducted using a GC Trace 1300 fitted with a split-splitless injector and column DB-5MS (60m \times 0.25 mm (i.d.), with film thickness 0.1 μm , non-polar stationary phase of 5 % phenyl and 95 % methyl silicone), using helium as a carrier gas (2 mL min^{-1}). The GC oven was programmed after 1 min from $60\text{ }^\circ\text{C}$ to $170\text{ }^\circ\text{C}$ at $6\text{ }^\circ\text{C min}^{-1}$, then from $170\text{ }^\circ\text{C}$ to $315\text{ }^\circ\text{C}$ at $2.5\text{ }^\circ\text{C min}^{-1}$ and held at $315\text{ }^\circ\text{C}$ for 15 min. The eluent from the GC was transferred directly via a transfer line ($320\text{ }^\circ\text{C}$) to the electron impact source of a Thermoquest ISQMS single quadrupole mass spectrometer. Typical operating conditions were: ionisation potential 70 eV; source temperature $215\text{ }^\circ\text{C}$; trap current 300 μA . Mass data were collected at a resolution of 600, cycling every second from 50 to 600 Da and were processed using Xcalibur software.

Compounds were identified either by comparison of their mass spectra and relative retention indices with those available in the literature, and/or by comparison with authentic standards. Shorthand notations of fatty acids and alcohols follows the IUPAC (International Union of Pure and Applied Chemistry, <http://www.iupac.org>) systematic nomenclature ‘n-x’ notation. Quantitative data were calculated by comparison of peak areas of the internal standard with those of the compounds of interest, using the total ion current (TIC) chromatogram. The relative response factors of the analytes were determined individually for 36 representative fatty acids and sterols using authentic standards. Response factors for analytes where standards were unavailable were assumed to be identical to those of available compounds of the same class.

Total lipid concentrations were expressed relative to zooplankton dry weight and nitrogen biomass (mg g N^{-1}). Nitrogen biomass was chosen over carbon biomass as amino acids/proteins are more representative of metabolically-active tissues than carbon, particularly in lipid-rich species (Ikeda, 1988; Ventura, 2006).

2.4. Data analysis

The relationships between $\delta^{15}\text{N}$ and depth, $\delta^{15}\text{N}$ of zooplankton and

$\delta^{15}\text{N}$ of POM and fatty acid/alcohol compositions with depth were investigated using linear regression. To deal with differences in individual compound concentrations between zooplankton taxa/POM samples, quantitative data (individual fatty acids/alcohols) were converted to relative abundances (mol%) of total identified lipid. Relative abundances for each lipid class were also calculated by summing the concentrations (nmol) of individual moieties into their respective classes and dividing each lipid class by the total lipid concentration of the individual zooplankton. The relationship between 18:1(n-9) and depth was investigated using linear regression. This fatty acid was of particular interest, as it is biosynthesized by animals (Dalsgaard et al., 2003), but not phytoplankton, and is therefore representative of zooplankton-sourced materials to the particle pool. The influence of POM size fraction ($<53\text{ }\mu\text{m}$ vs. $>53\text{ }\mu\text{m}$), time of collection (P3A/P3B/P3C) and sampling depth on the composition (mol%) of the 13 most abundant fatty acids, which made up $>80\%$ of total fatty acid composition, were examined using redundancy analysis (RDA). The influence of zooplankton taxa and time of collection (P3B and P3C; no P3A zooplankton lipid data available) on the composition (mol%) of fatty acids were also examined using RDA analysis. The significance of individual model terms were determined using a permuted ($n = 9999$) forward selection procedure (Mayor et al., 2013). Fatty acids that accounted for $<3\%$ of total fatty acids and missing values for individual taxa were excluded from the RDA analysis as RDA sees zero values as similar (Zuur et al., 2007). Fatty acids with single missing values were imputed by taking a mean of all other values for the individual taxon and fatty acid. Additional RDA analyses were conducted to investigate whether the compositions of lipid classes were influenced by the different taxa. All statistical analyses were conducted in the R v4.1.3 programming environment (R Core Team, 2022) using the ‘Vegan’ package (Oksanen et al., 2020). Data obtained at the P3 station during each visit is summarised in Table 1.

3. Results

3.1. Stable isotope compositions

The $\delta^{15}\text{N}$ signatures of POM at P3 ranged between 1.24 ‰ and 8.22 ‰ and became progressively ^{15}N -enriched with depth (ANOVA, $F = 25.1_{(1,18)}$, $p < 0.001$; Fig. 1). POM $\delta^{15}\text{N}$ values did not change significantly between the three visits to P3 (ANOVA, $F = 0.130_{(2,17)}$, $p = 0.879$).

The mean $\delta^{15}\text{N}$ signatures of the zooplankton varied between 3.50 ‰ and 8.97 ‰, with the lowest being in the salp *S. thompsoni* and the copepod *R. gigas*, followed by the amphipod *T. gaudichaudii* and copepod *C. acutus*, increasing to euphausiids and chaetognaths and the copepod *Paraeuchaeta* spp. which was most enriched in ^{15}N (Table 2; Supplementary Fig. S1). The $\delta^{15}\text{N}$ values of *T. gaudichaudii* and *R. gigas* were both correlated with POM $\delta^{15}\text{N}$ values ($F \geq 12.76_{(1, \geq 11)}$, $p < 0.001$ in both cases), and depth ($F = 14.26_{(1,11)}$, $p = 0.003$ and $F = 11.76_{(1,17)}$, $p = 0.003$ respectively) whereas all other species were not ($p > 0.05$ in all cases). *T. gaudichaudii* $\delta^{15}\text{N}$ values increased with depth ($y = 45.7x - 199.5$; $R^2 = 0.56$) whereas those for *R. gigas* decreased ($y = -106.5x + 734.6$; $R^2 = 0.41$) (Fig. 2). Estimated trophic levels ranged from 3.61 to 5.46 (Fig. 3). The lowest trophic levels were found in *S. thompsoni* and *R. gigas*, followed by *T. gaudichaudii*, *Thysanoessa* spp., Chaetognatha,

Table 1

Summary of particulate organic matter (POM) and zooplankton data available at each visit of the P3 station in the Scotia Sea, South Georgia.

	P3A	P3B	P3C
POM lipid data	✓	✓	✓
POM stable isotope data	✓	✓	✓
Zooplankton lipid data	X	✓	✓
Zooplankton stable isotope data	X	✓	✓

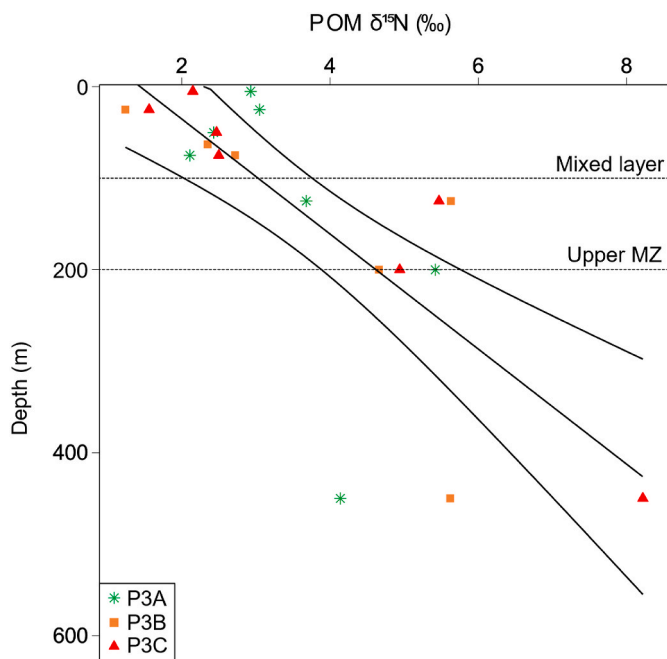


Fig. 1. $\delta^{15}\text{N}$ signatures of particulate organic matter (POM) in relation to sampling depth at station P3 (P3A + P3B + P3C) in the Scotia Sea. The regression line indicates a statistically significant ($p < 0.05$) relationship between $\delta^{15}\text{N}$ of POM and depth. $y = -90.55x (\pm 50.91) + 62.88 (\pm 12.55)$. $R^2 = 0.58$. Standard errors are illustrated either side of the regression line and given in brackets next to the equation coefficients. Horizontal dotted lines indicate the boundaries of the mixed layer depth (0–95 m) and the upper mesopelagic zone (MZ) (96–200 m) (Giering et al., 2023).

E. triacantha and lastly *Paraeuchaeta* spp.

3.2. Fatty acid signatures of particulate organic matter

The lipid composition of POM is described in Preece et al. (Submitted). Briefly, the fatty acid composition (mol%) of the $<53 \mu\text{m}$ POM was dominated by 20:5(n-3), followed by 16:1(n-7) and 22:6(n-3) (40.7 ± 6.4 , 14.5 ± 5.1 and 11.6 ± 5.8 mol% respectively; Table 3). The fatty acid composition of the $>53 \mu\text{m}$ POM was dominated by 16:1(n-7), 18:1(n-9) and 20:5(n-3) (26.8 ± 9.3 , 15.8 ± 10.7 and 11.2 ± 11.4 mol% respectively; Table 3). The percentage of the 18:1(n-9) fatty acid in POM increased with depth (Fig. 4) in both $<53 \mu\text{m}$ and $>53 \mu\text{m}$ size fractions ($F = 8.20_{(1,20)}$, $p = 0.009$; $F = 23.6_{(1,20)}$, $p < 0.001$, respectively). Other fatty acids with percentage compositions that increased with depth included 18:2(tr-9) for both size fractions ($<53 \mu\text{m}$: $F = 7.77_{(1,20)}$, $p = 0.011$, $R^2 = 0.28$; $>53 \mu\text{m}$: $F = 6.16_{(1,20)}$, $p = 0.022$, $R^2 = 0.24$) and 18:0 for the $<53 \mu\text{m}$ size fraction ($F = 42.6_{(1,20)}$, $p < 0.001$, $R^2 = 0.68$; Supplementary Fig. S2; Table S3). The percentage composition of 14:0 decreased with increasing depth in the $>53 \mu\text{m}$ size fraction ($F = 7.54_{(1,20)}$, $p = 0.012$, $R^2 = 0.27$; Supplementary Fig. S2; Table S3). No other POM fatty acid changed with depth (Supplementary Table S3).

The fatty acid composition of the POM varied as a function of particle size ($<53 \mu\text{m}$ or $>53 \mu\text{m}$) and sampling depth (RDA, $F = 13.67_{(1,42)}$, $p < 0.001$ and $F = 6.34_{(1,42)}$, $p < 0.001$ respectively; Fig. 5; see also Preece et al., Submitted). Including time of collection (P3A/P3B/P3C) had no effect on the model fit ($F = 1.73_{(2,42)}$, $p = 0.073$) and was therefore excluded from the model. The final RDA model explained 35.4 % of the total variance in the data, with the first and second axes accounting for 28.1 % and 7.32 % of the overall variability, respectively. Particle size was ordinated across the first axis, with $<53 \mu\text{m}$ and $>53 \mu\text{m}$ POM generally having positive and negative values on this axis, respectively. The PUFAs 20:5(n-3), 22:6(n-3) and 16:4, were more closely associated with the $<53 \mu\text{m}$ fraction. All other fatty acids were more closely associated to the $>53 \mu\text{m}$ POM.

Table 2

Dry weight (DW, mg), organic nitrogen content per DW (mg N), organic carbon content per DW (mg C), mg of lipid to DW content (mg lipid g DW⁻¹), lipid to organic nitrogen content (mg g N⁻¹) and lipid to organic carbon content (mg g C⁻¹) and $\delta^{15}\text{N}$ signatures of zooplankton (mean \pm standard deviation) sampled at the P3 (P3B + P3C) station in the Scotia Sea. One outlier value in the lipids data was removed when calculating the means for *T. gaudichaudii* due to the value being an order of magnitude larger than the rest of the data. The number of replicates (n) for lipid analyses are indicated for each taxa in the top row of each station visit. Replicate sizes for the stable isotope data are indicated within the $\delta^{15}\text{N}$ row for each station visit.

		<i>Calanoides acutus</i>	Chaetognatha	<i>Euphausia triacantha</i>	<i>Paraeuchaeta</i> spp.	<i>Rhincalanus gigas</i>	<i>Salpa thompsoni</i>	<i>Themisto gaudichaudii</i>	<i>Thysanoessa</i> spp.
	n	3	3	3	0	4	1	0	2
P3B	mg DW	1.9 \pm 1.1	7.4 \pm 5.0	76.6 \pm 43.7	–	3.1 \pm 1.2	4.4	–	23.4 \pm 6.2
	mg N	0.1 \pm 0.06	0.4 \pm 0.1	5.1 \pm 3.2	–	0.2 \pm 0.09	0.2	–	2.2 \pm 0.4
	mg C	1.1 \pm 0.7	1.6 \pm 0.4	40.8 \pm 23.6	–	1.7 \pm 0.7	0.8	–	9.1 \pm 2.9
	mg lipids g DW ⁻¹	516.9 \pm 117.5	118.8 \pm 52.3	100.0 \pm 38.5	–	427.3 \pm 28.6	43.2	–	154.0 \pm 145.0
	mg lipids g N ⁻¹	30.6 \pm 6.5	8.9 \pm 5.8	6.4 \pm 1.5	–	25.8 \pm 4.7	1.70	–	14.1 \pm 12.5
	mg lipids g C ⁻¹	289.8 \pm 61.1	37.1 \pm 25.9	54.9 \pm 31.5	–	231.6 \pm 25.0	8.0	–	60.9 \pm 59.3
	$\delta^{15}\text{N}$ (‰)	5.4 \pm 1.4 (n = 3)	6.2 \pm 0.6 (n = 9)	6.3 \pm 0.9 (n = 12)	7.3 (n = 1)	4.9 \pm 0.3 (n = 3)	5.0 \pm 1.1 (n = 10)	5.4 \pm 0.1 (n = 4)	6.3 \pm 0.7 (n = 16)
P3C	n	3	4	2	1	3	1	2	3
	mg DW	3.0 \pm 0.4	6.5 \pm 9.6	45.6 \pm 8.1	1.7	4.8 \pm 1.4	12.8	6.4 \pm 4.1	43.5 \pm 52.5
	mg N	0.2 \pm 0.02	0.6 \pm 0.9	4.8 \pm 0.1	0.2	0.3 \pm 0.08	0.1	0.5 \pm 0.3	4.8 \pm 6.3
	mg C	1.7 \pm 0.1	2.4 \pm 3.5	19.6 \pm 3.2	0.8	2.6 \pm 0.9	0.7	2.5 \pm 1.7	17.5 \pm 21.9
	mg lipids g DW ⁻¹	438.7 \pm 106.4	61.9 \pm 15.3	155.5 \pm 16.6	194.1	276.0 \pm 42.8	28.3	122.4 \pm 36.1	107.8 \pm 66.5
	mg lipids g N ⁻¹	31.5 \pm 5.9	5.8 \pm 1.5	16.9 \pm 4.4	18.4	18.5 \pm 1.0	0.3	9.2 \pm 2.4	11.1 \pm 7.9
	mg lipids g C ⁻¹	245.8 \pm 48.4	23.7 \pm 7.1	67.2 \pm 8.3	93.4	152.7 \pm 31.4	1.5	46.4 \pm 10.7	42.6 \pm 29.1
$\delta^{15}\text{N}$ (‰)	7.0 \pm 1.7 (n = 5)	7.1 \pm 0.4 (n = 6)	7.2 \pm 0.8 (n = 10)	7.7 \pm 1.5 (n = 2)	5.1 \pm 0.8 (n = 16)	5.0 \pm 0.8 (n = 9)	6.2 \pm 0.8 (n = 9)	6.2 \pm 0.7 (n = 14)	

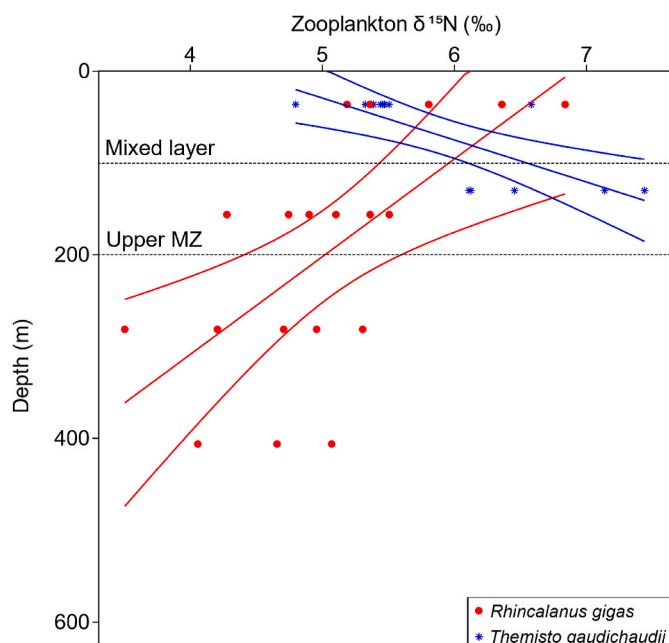


Fig. 2. $\delta^{15}\text{N}$ signatures of *Rhincalanus gigas* and *Themisto gaudichaudii* in relation to depth at station P3 (P3B + P3C) in the Scotia Sea. Depth values represent mean depth of the net from which specimens were collected from. *T. gaudichaudii* were collected in the upper 250 m, using either a RMT 25 net sampling between 10 and 250 m or a MOCNESS net sampling 10–62 m (see [Supplementary Fig. S2](#) for details). Insufficient *T. gaudichaudii* were collected at depths beyond 250 m for analysis. The regression lines indicate a statistically significant ($p < 0.05$) relationship between the $\delta^{15}\text{N}$ values of the zooplankton and depth (*T. gaudichaudii* = blue: $y = 0.779x (\pm 0.218) + 4.106 (\pm 0.536)$ ($R^2 = 0.54$); *R. gigas* = red: $y = -0.238x (\pm 0.066) + 6.268 (\pm 0.364)$ ($R^2 = 0.44$). Standard error values for the equation coefficients are given in brackets. Only taxa with significant linear relationships are plotted. Horizontal dotted lines indicate the boundaries of the mixed layer depth (0–95 m) and the upper mesopelagic zone (MZ) (96–200 m) ([Giering et al., 2023](#)).

3.3. Fatty acid and alcohol signatures of zooplankton

Fatty acids made up > 60 mol% of the total lipids within each taxa sampled ([Table 5](#)). The relative abundances of monosaturated fatty acids (MUFAs) and PUFAs were similar across taxa, with higher amounts of PUFAs compared to MUFAs, apart from *Paraeuchaeta* spp., which contained a greater amount of MUFAs (49.4 mol%) and less PUFAs (9.2 mol %; note only one *Paraeuchaeta* specimen was sampled; [Table 5](#)). The dominant MUFAs in all taxa were 16:1(n-7) and 18:1(n-9) (as well as 20:1(n-9) in *C. acutus*). 20:5(n-3) and/or 22:6(n-3) were the most abundant PUFA(s) in all taxa ([Table 6](#)). Other PUFAs included 16:4, 18:2 (n-6) and 18:3(n-5). Saturated fatty acids (SFAs), mainly 14:0 and 16:0, made up between 15 and 27 mol% of total lipids for all except the three copepod species (*C. acutus*, *R. gigas* and *Paraeuchaeta* spp.), where total SFAs accounted for < 8 mol% ([Table 5](#)). All non-copepod zooplankton taxa had low or moderate contributions of fatty alcohols (< 12 %; [Table 5](#)). By contrast, fatty alcohols in the three copepod species represented > 25 % of the total lipid pool. *C. acutus* alcohols were dominated by unsaturated compounds, specifically ALC-20:1 and ALC-22:1, whereas *R. gigas* alcohols were dominated by saturated alcohols, predominately ALC-14:0 and ALC-16:0 ([Table 7](#)). *Paraeuchaeta* spp. had a more equal distribution of saturated and unsaturated alcohols.

3.4. RDA analysis of zooplankton lipid data

Taxon identity explained 77.2 % of the total variance in the zooplankton lipid class composition data (RDA, $F = 13.55_{(7,28)}$, $p < 0.001$; [Fig. 6](#)), with the first and second axes accounting for 36.0 % and

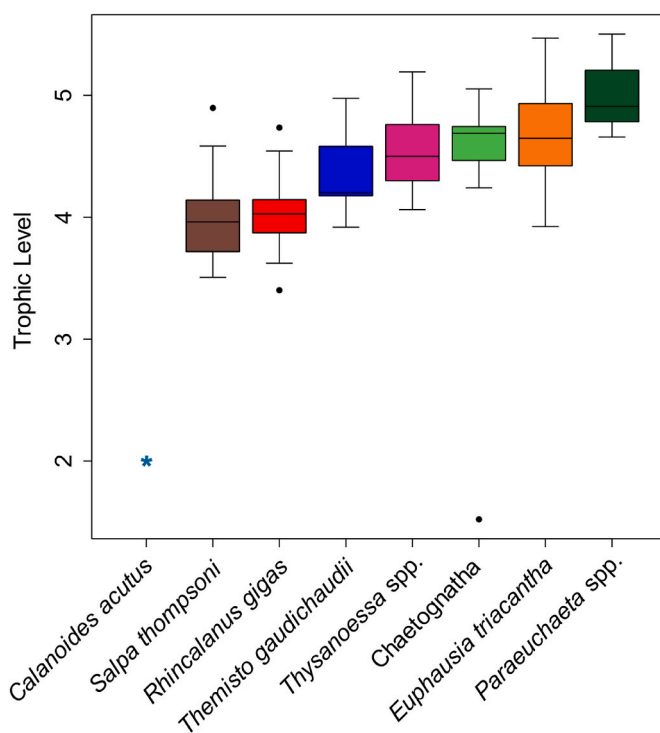


Fig. 3. Estimated trophic level for the 8 zooplankton taxa at station P3 (P3B + P3C) in the Scotia Sea. The boxplot represents the minimum, maximum, median, first quartile and third quartile values. Circles represent outliers. Trophic level was calculated from $\delta^{15}\text{N}$, assuming a trophic enrichment factor of 2.5 ‰ per trophic level. The baseline consumer $\delta^{15}\text{N}$ signature used to calculate trophic levels was based on the mean $\delta^{15}\text{N}$ of *Calanoides acutus* ($\delta^{15}\text{N} = 6.38 \pm 1.73$; asterisk) and a baseline consumer trophic level = 2.0 (asterisk). *C. acutus* $\delta^{15}\text{N}$ signatures were not affected by sampling depth ($F = 0.002_{(1,6)}$, $p = 0.963$).

18.1 % of the variability, respectively. Including time of collection (P3B/P3C) did not improve the model fit ($F = 0.599_{(1,34)}$, $p = 0.670$) and was therefore omitted. There was a distinct separation of the three copepods from the rest of the zooplankton. Copepods had strong negative loadings on the first axis and associations with alcohols, unsaturated alcohols and MUFAs, while all other species had positive loadings on the first axis and associations with sterols and SFAs. *R. gigas* was strongly associated with saturated alcohols, whereas *C. acutus* and *Paraeuchaeta* spp. were associated with unsaturated alcohols and MUFAs.

Taxon identity explained 73.0 % of the total variance in the zooplankton fatty acid compositional data (RDA, $F = 10.8_{(7,28)}$, $p < 0.001$), with the first and second axes accounting for 32.7 % and 21.9 % of the variability, respectively ([Fig. 7](#)). Including time of collection (P3B and P3C) did not improve the model fit ($F = 0.467_{(1,34)}$, $p = 0.856$) and was therefore omitted. *E. triacantha*, Chaetognatha, *Thysanoessa* spp., *S. thompsoni* and *T. gaudichaudii* grouped together and were positively associated with the fatty acids 14:0, 18:1(tr-9), 16:0 and 22:6(n-3), 14:0 and 22:1(n-9). Chaetognatha demonstrated a range of both strong positive and negative loadings on the second axis, with some individuals being closely associated to 22:1(n-9) and others to 18:1(tr-9).

The three copepod species were ordinated away from the other taxa and each other, with *C. acutus* having strong negative loadings on the first axis and positive loadings on the second axis. *R. gigas* had strong negative loadings on both the first and second axes. *Paraeuchaeta* spp. had a strong negative loading on the second axis. *C. acutus* was particularly associated with 20:1(n-9), with the composition of this MUFA being higher in *C. acutus* (12.5 mol%) compared to all other species (< 6 mol%; [Table 6](#)). *C. acutus* was also closely associated with the PUFAs 20:5(n-3) and 18:3(n-6), and to a lesser extent 22:1(n-11) and 20:4. *R. gigas* was particularly associated with the short-chained fatty acids

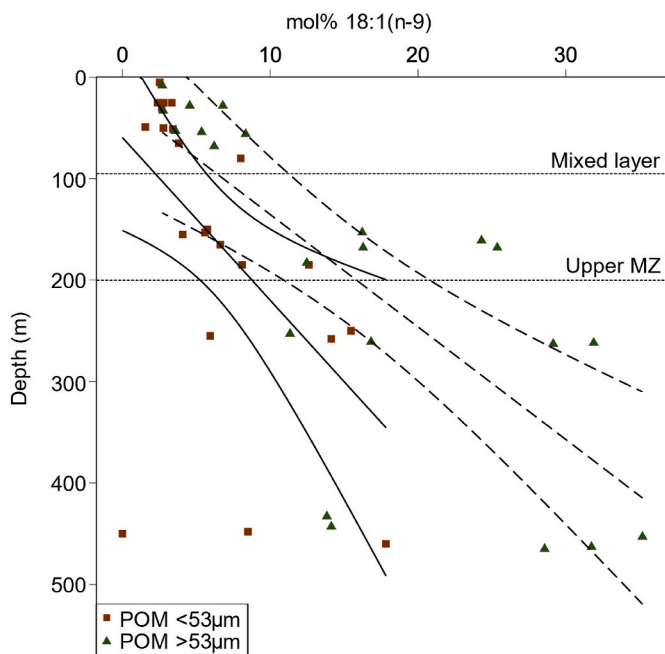


Fig. 4. Relationships between depth and the relative abundance of the biomarker 18:1(n-9) (mol%) fatty acid in the <53 µm (filled squares) and >53 µm (filled triangles) size-fractions of particulate organic matter (POM) sampled at station P3 (P3A + P3B + P3C) in the Scotia Sea. This fatty acid is biosynthesized by animals (Dalsgaard et al., 2003), but not phytoplankton, and is therefore representative of zooplankton-sourced materials to the particle pool and more reworked POM. The regression lines indicate statistically significant ($p < 0.05$) linear relationships. POM <53 µm (solid line): $y = 16.06x (\pm 5.61) + 59.44 (\pm 43.92)$ ($R^2 = 0.29$); POM >53 µm (dashed line): $y = 11.08x (\pm 2.28) + 24.41 (\pm 43.19)$ ($R^2 = 0.54$). Standard errors are illustrated either side of the regression line and given in brackets next to the equation coefficients. Horizontal dotted lines indicate the boundaries of the mixed layer depth (0–95 m) and the upper mesopelagic zone (MZ) (96–200 m) (Giering et al., 2023).

16:4 and 16:1(n-7). *Paraeuchaeta* spp. was strongly associated with 18:1(n-9) and 16:1(n-7).

4. Discussion

4.1. Lipid content of particulate organic matter

The occupation of station P3 was characterised by a phytoplankton bloom dominated by large diatoms, with live, intact cells at depths within and below the epipelagic zone (Manno et al., 2022; Ainsworth et al., 2023). Lipid composition data of POM are originally presented and discussed in detail in Preece et al. (Submitted) and reiterated here to facilitate the interpretation of the zooplankton data. The dominance of diatom markers 20:5(n-3) and 16:1(n-7) in both POM size fractions throughout the water column down to 500 m (Table 3; Preece et al., Submitted) is entirely consistent with the occurrence of diatoms at depth. The differences in the fatty acid compositions of the two particle size classes (Fig. 5) were driven by the increased relative abundances of the PUFAs, 20:5(n-3) and 22:6(n-3), in the <53 µm samples, and increased relative abundances of 18:1(n-9), 18:2(tr-9), and 20:1(n-9) in the >53 µm samples. The MUFA 18:1(n-9), which is biosynthesized by zooplankton (Dalsgaard et al., 2003), contributed on average 15.8 mol% to the >53 µm POM fatty acids, compared to 6.3 % in the <53 µm size fraction (Table 3) and increased in relative concentration with increasing depth (Fig. 4). Similar contributions of 18:1(n-9) in POM have previously been observed (Richoux, 2011), and its increased relative abundance with depth suggests that zooplankton-sourced materials become increasingly more important in midwater particle pools

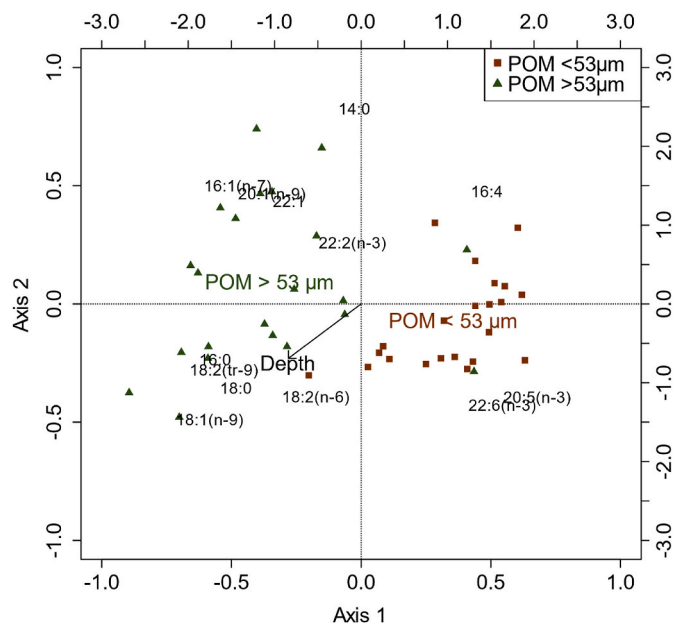


Fig. 5. Fatty acid composition (mol%) of size-fractionated particulate organic matter (POM) from station P3 (P3A + P3B + P3C) in the Scotia Sea. Redundancy analysis distance triplot of the proportional abundance of each fatty acid for the two particle sizes and the continuous variable depth. Each single point refers to a single sample of POM. The effect of depth is plotted as a vector (solid black line). The primary and secondary sets of axes relate to the individual samples and fatty acid loadings, respectively.

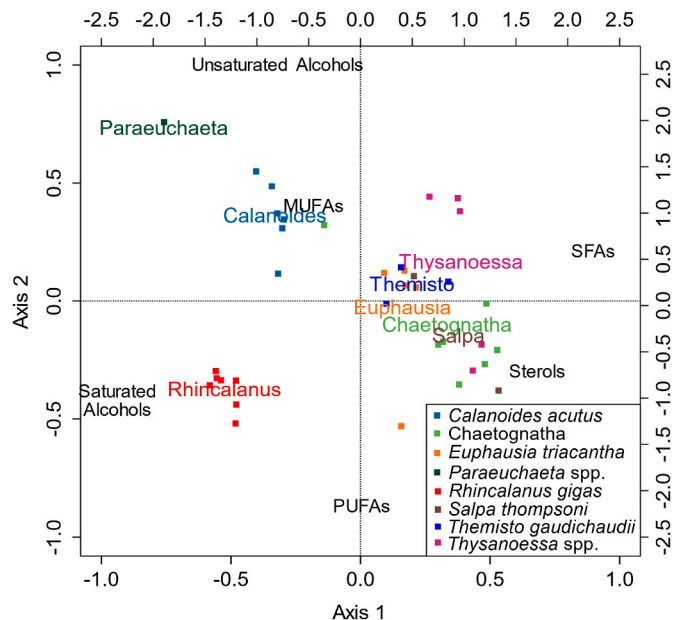


Fig. 6. Lipid class composition (mol%) of the zooplankton taxa from station P3 (P3B + P3C) in the Scotia Sea. Redundancy analysis distance triplot of the proportional abundance of each lipid class in each sampled zooplankton taxa and 6 different lipid classes. The primary and secondary sets of axes relate to the individual zooplankton samples and lipid class loadings, respectively. Each single point refers to an individual taxon replicate.

(Sheridan et al., 2002). The presence of 18:1(n-9) within the large POM fraction may moreover be attributed to live particle associated copepods (PAC) too small to be removed from the SAPs filters, such as Oithonidae and Oncaidae (<1 mm). These copepods produce large lipid stores that are dominated by 18:1(n-9) as well as the fatty alcohols ALC-14:0 and

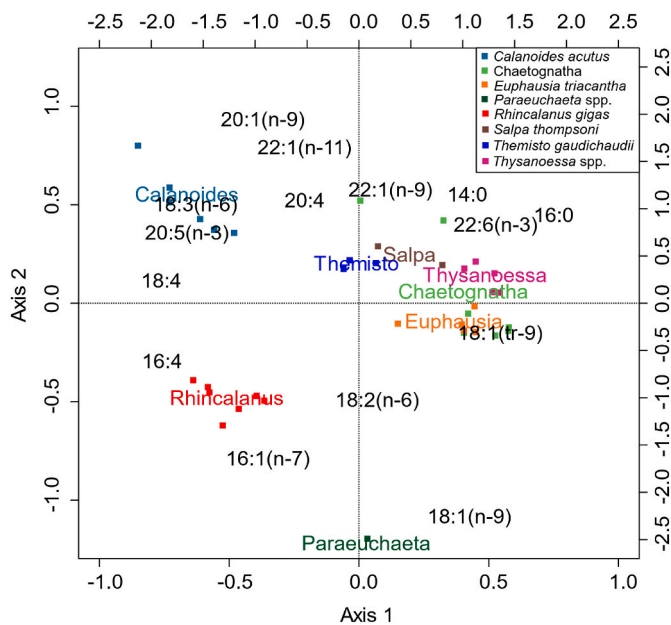


Fig. 7. Fatty acid composition (mol%) of the zooplankton taxa from station P3 (P3B + P3C) in the Scotia Sea. Redundancy analysis distance triplot of the proportional abundance of fatty acids in each sampled zooplankton taxa and 16 fatty acids. The primary and secondary sets of axes relate to the individual zooplankton samples and fatty acid loadings, respectively. Each single point refers to an individual taxon replicate.

ALC-16:0 and to a lesser extent ALC-20:1(n-9) and ALC-22:1(n-11) (Kattner et al., 2003). Indeed, there was an increased contribution of copepod lipids, largely unsaturated alcohols, to the >53 μm POM size fraction in the upper mesopelagic possibly derived from *Oithona* (Table 4; Supplementary Fig. S3; up to 35 %, Preece et al., Submitted). This is consistent with the idea that small PACs are important in reworking and attenuating sinking POM in the upper mesopelagic (Mayor et al., 2014, 2020; Koski et al., 2020).

Table 3

Fatty acid composition (mol%, mean ± standard deviation) of <53 μm and >53 μm POM throughout epi- and mesopelagic waters at station P3 (P3A + P3B + P3C) in the Scotia Sea, focusing on the 13 most abundant fatty acids (making up > 80% of fatty acid composition). Fatty acid values were averaged across 5 depth bins. The number of replicates (n) is indicated for each depth bin. Data reproduced from Preece et al., Submitted.

Depth bin (m)	POM <53 μm						POM >53 μm					
	5–30 n = 5	49–80 n = 5	150–185 n = 6	250–258 n = 3	448–460 n = 3	Mean n = 22	5–30 n = 4	45–65 n = 4	150–180 n = 5	250–260 n = 4	430–462 n = 5	Mean n = 22
14:0	2.9 ± 1.6	3.1 ± 0.3	1.8 ± 0.5	1.3 ± 0.6	2.1 ± 0.7	2.2 ± 1.0	4.4 ± 3.3	6.3 ± 3.4	2.2 ± 2.1	2.3 ± 0.7	1.5 ± 1.2	3.2 ± 2.8
16:0	2.6 ± 0.9	6.4 ± 8.2	3.9 ± 1.4	3.7 ± 0.8	8.4 ± 1.2	4.8 ± 4.2	7.8 ± 6.5	9.4 ± 4.7	4.9 ± 3.2	8.7 ± 3.0	8.7 ± 3.7	7.8 ± 4.2
18:0	0.2 ± 0.0	0.3 ± 0.1	0.5 ± 0.3	0.8 ± 0.4	3.7 ± 1.9	0.9 ± 1.3	3.1 ± 4.2	1.4 ± 0.5	1.4 ± 0.6	3.1 ± 1.1	3.9 ± 2.1	2.6 ± 2.2
16:1(n-7)	17.1 ± 3.6	13.1 ± 7.1	11.4 ± 6.5	15.1 ± 1.9	17.5 ± 2.6	14.5 ± 5.1	26.1 ± 11.8	36.7 ± 7.0	21.5 ± 10.4	22.8 ± 6.2	28.0 ± 4.2	26.8 ± 9.3
18:2(n-6)	1.9 ± 1.4	3.0 ± 0.3	2.8 ± 1.2	3.4 ± 1.3	3.5 ± 0.9	2.9 ± 1.1	2.4 ± 1.1	2.3 ± 1.4	2.6 ± 0.4	4.9 ± 5.0	4.1 ± 1.2	3.3 ± 2.3
18:1(n-9)	2.8 ± 0.4	2.4 ± 0.9	6.0 ± 1.4	11.2 ± 4.1	8.8 ± 8.9	6.3 ± 4.8	4.2 ± 1.9	5.9 ± 2.0	18.9 ± 5.6	22.3 ± 9.9	24.7 ± 10.1	15.8 ± 10.7
18:2(tr-9)	1.9 ± 0.8	2.7 ± 0.8	3.2 ± 0.4	4.8 ± 1.5	4.1 ± 1.1	3.3 ± 1.4	4.2 ± 3.7	5.5 ± 2.4	4.6 ± 2.1	6.8 ± 1.4	8.0 ± 3.2	5.9 ± 2.9
20:5(n-3)	41.0 ± 5.2	40.4 ± 3.1	47.7 ± 4.6	37.3 ± 5.7	34.5 ± 7.0	40.7 ± 6.4	11.7 ± 12.6	5.3 ± 6.2	19.1 ± 16.0	13.9 ± 9.6	5.6 ± 6.9	11.2 ± 11.4
20:1(n-9)	2.4 ± 2.8	0.2 ± 0.1	0.3 ± 0.2	2.2 ± 3.2	0.7 ± 0.3	1.2 ± 2.0	0.2 ± 0.4	5.5 ± 6.5	6.9 ± 3.9	5.8 ± 2.5	3.1 ± 1.7	4.4 ± 4.0
22:6(n-3)	9.1 ± 6.4	11.7 ± 6.6	13.3 ± 7.9	13.9 ± 3.8	10.3 ± 3.1	11.9 ± 5.8	2.5 ± 4.1	0.6 ± 0.6	5.2 ± 7.5	2.2 ± 4.40	1.1 ± 1.7	2.4 ± 4.4
22:1	2.8 ± 3.4	0.6 ± 0.2	0.9 ± 0.9	0.6 ± 0.6	3.6 ± 3.1	1.6 ± 2.2	6.5 ± 9.9	5.1 ± 5.5	8.1 ± 6.8	3.7 ± 2.5	3.3 ± 2.6	5.4 ± 5.7

4.2. Trophic ecology of the zooplankton

The calculated zooplankton trophic levels ranged between 3.6 and 5.5 (Fig. 3), suggesting a degree of trophic overlap within the zooplankton food web. We observed a subtle continuous, rather than stepwise, increase in trophic level, with *S. thompsoni* being at the lowest and the carnivorous copepod *Paraeuchaeta* spp. at the highest trophic level, respectively. The isotopic signatures of copepods were broadly aligned with their trophic ecology inferred from the fatty acid analysis. Indeed, the high contributions of 16:1(n-7) and 20:5(n-3) in *C. acutus* and *R. gigas* suggest diatoms to be a dominant source of food and supports the idea that these species are broadly herbivorous (Kattner et al., 1994; Kates and Volcani, 1966; Ward et al., 1996; Falk-Petersen et al., 1999). The top trophic position of *Paraeuchaeta* spp. aligns with previous studies describing this species as predatory (Hopkins, 1985; Øresland, 1991; Øresland and Ward, 1993). Isotopic and fatty acid data for the euphausiids were broadly consistent with these species being omnivores (Phleger et al., 1998; Falk-Petersen et al., 1999; Richoux, 2011), as suggested by the presence of both phytoplankton and calanoid biomarkers. The high percent contributions of ALC-20:1 and ALC-22:1 in both species moreover suggests their feeding on *C. acutus* (Table 7), the most abundant copepod. Other Southern Ocean calanoid species such as *Calanus propinquus* and *Calanus similimus* also biosynthesize the calanoid biomarkers 20:1(n-9) and 22:1(n-11) (Hagen et al., 1993; Ward et al., 1996), however, these species were present in negligible amounts in nets during the study period (Cook et al., 2023).

The δ¹⁵N and trophic position of Chaetognatha were similar to those of the omnivorous euphausiids, despite them being considered active predators (Pakhomov et al., 1999). Chaetognatha fatty acid composition was consistent with other studies; 22:6(n-3) and 20:5(n-3), and to a lesser extent 16:0, 16:1(n-7) and 18:1(n-9), dominate the composition of Antarctic chaetognaths (Kruse et al., 2010). The calanoid biomarker 20:1(n-9) was observed in high proportions in one of the seven individuals sampled and was also abundant in alcohol form (Table 7), suggesting feeding on *C. acutus*. The wide array of fatty acids present in Chaetognatha may reflect their known behaviour as opportunistic feeders (Froneman and Pakhomov, 1998; Froneman et al., 1998).

The fatty acids of *T. gaudichaudii* were dominated by 20:5(n-3), 16:0,

Table 4

Fatty alcohol composition (mol%, mean \pm standard deviation) of $<53 \mu\text{m}$ and $>53 \mu\text{m}$ POM throughout epi- and mesopelagic waters at station P3 (P3A + P3B + P3C) in the Scotia Sea, focusing on the 4 most abundant fatty alcohols. Fatty alcohol values were averaged across 5 depth bins. The number of replicates (n) is indicated for each depth bin. Data reproduced from Preece et al., Submitted.

Depth bin (m)	POM $<53 \mu\text{m}$					Mean = 22	POM $>53 \mu\text{m}$					Mean = 22
	5–30 n = 5	49–80 n = 5	150–185 n = 6	250–258 n = 3	448–460 n = 3		5–30 n = 4	45–65 n = 4	150–180 n = 5	250–260 n = 4	430–462 n = 5	
ALC-14:0	1.1 \pm 0.9	2.6 \pm 3.0	1.5 \pm 1.1	2.5 \pm 3.0	1.0 \pm 0.9	1.7 \pm 1.9	1.3 \pm 1.8	1.1 \pm 0.8	6.9 \pm 5.4	4.1 \pm 2.7	4.2 \pm 3.6	3.7 \pm 3.8
ALC-16:0	1.1 \pm 1.1	2.8 \pm 3.4	2.8 \pm 3.2	4.5 \pm 4.1	2.1 \pm 1.2	2.5 \pm 2.8	1.3 \pm 2.1	1.1 \pm 1.2	10.4 \pm 4.9	7.0 \pm 4.3	10.3 \pm 8.7	6.4 \pm 6.3
ALC-20:1	3.7 \pm 4.8	0.6 \pm 0.7	1.6 \pm 2.7	0.9 \pm 1.2	0.3 \pm 0.5	1.6 \pm 2.8	–	1.1 \pm 0.8	9.9 \pm 7.4	7.6 \pm 5.0	4.2 \pm 1.7	4.8 \pm 5.4
ALC-22:1	1.7 \pm 2.4	0.3 \pm 0.3	0.1 \pm 0.1	0.1 \pm 0.2	–	0.5 \pm 1.3	2.1 \pm 4.1	0.1 \pm 0.2	3.9 \pm 2.8	1.6 \pm 1.9	0.1 \pm 0.2	1.6 \pm 2.6

Table 5

Lipid class composition (mol%, mean \pm standard deviation) of each zooplankton taxa sampled at station P3 (P3B + P3C) in the Scotia Sea. Saturated-, mono-unsaturated- and polyunsaturated-fatty acids are abbreviated as SFA, MUFA and PUFA respectively. The number of replicate samples (n) is indicated for each taxon. Replicate samples of *C. acutus* each contained 5 individuals. Replicate samples of *R. gigas* each contained 2 individuals. All other taxa replicates contained 1 individual per replicate.

	<i>Calanoides acutus</i> n = 6	Chaetognatha n = 7	<i>Euphausia triacantha</i> n = 5	<i>Paraeuchaeta</i> spp. n = 1	<i>Rhincalanus gigas</i> n = 7	<i>Salpa thompsoni</i> n = 2	<i>Themisto gaudichaudii</i> n = 3	<i>Thysanoessa</i> spp. n = 5
SFA	7.4 \pm 0.5	15.5 \pm 4.3	20.5 \pm 3.5	2.2	2.5 \pm 0.7	21.0 \pm 4.1	20.1 \pm 3.4	26.9 \pm 5.5
Branched Acids	0.2 \pm 0.2	0.5 \pm 0.2	1.9 \pm 0.7	0.6	0.0 \pm 0.0	1.4 \pm 0.4	0.9 \pm 0.5	0.6 \pm 0.4
MUFA	23.7 \pm 2.6	26.4 \pm 2.9	22.5 \pm 4.8	49.4	21.9 \pm 1.8	13.6 \pm 5.3	25.6 \pm 2.7	17.1 \pm 2.6
PUFA	32.4 \pm 6.6	45.4 \pm 7.4	43.0 \pm 10.9	9.2	49.9 \pm 3.8	46.7 \pm 11.8	42.1 \pm 3.5	40.2 \pm 11.1
Saturated Alcohols	8.4 \pm 0.7	1.5 \pm 1.7	5.1 \pm 1.4	21.6	20.7 \pm 1.8	2.3 \pm 3.0	2.0 \pm 1.3	0.4 \pm 0.3
Unsaturated Alcohols	27.5 \pm 3.3	3.2 \pm 6.2	4.4 \pm 1.2	16.5	4.6 \pm 0.7	9.5 \pm 8.7	7.0 \pm 3.6	11.6 \pm 6.4
Sterols	0.3 \pm 0.2	7.4 \pm 3.4	2.3 \pm 0.3	0.5	0.6 \pm 0.2	5.5 \pm 0.7	2.4 \pm 1.2	3.2 \pm 2.5
Phytadienes	0.00	0.00	0.4 \pm 0.8	0.00	0.00	0.00	0.00	0.00
Total fatty acids	63.6 \pm 7.1	87.3 \pm 90.4	86.0 \pm 12.4	60.7	74.2 \pm 4.2	81.4 \pm 13.5	87.8 \pm 5.6	84.2 \pm 12.7
Total alcohols	36.0 \pm 3.3	4.8 \pm 6.5	9.5 \pm 1.8	38.1	25.2 \pm 1.8	11.8 \pm 9.2	8.9 \pm 3.8	12.0 \pm 6.5

Table 6

Fatty acid composition (mol% mean \pm standard deviation) of the 8 studied zooplankton taxa sampled at station P3 (P3B + P3C) in the Scotia Sea, focusing on the 15 most abundant fatty acids included in the RDA model. *The fatty acid 22:1 was tentatively assigned hereafter as 22:1(n-11) based on the knowledge of 22:1(n-11) being a fatty acid only biosynthesized by herbivorous calanoid copepods such as *C. acutus* (Hagen et al., 1993; Dalsgaard et al., 2003). The number of replicate samples (n) is indicated for each taxon. Replicate samples of *C. acutus* each contained 5 individuals. Replicate samples of *R. gigas* each contained 2 individuals. All other taxa replicates contained 1 individual per replicate.

	<i>Calanoides acutus</i> n=6	Chaetognatha n=7	<i>Euphausia triacantha</i> n=5	<i>Paraeuchaeta</i> spp. n=1	<i>Rhincalanus gigas</i> n=7	<i>Salpa thompsoni</i> n=2	<i>Themisto gaudichaudii</i> n=3	<i>Thysanoessa</i> spp. n=5
14:0	7.8 \pm 1.3	5.2 \pm 4.1	12.7 \pm 2.6	1.1	0.9 \pm 0.5	12.3 \pm 0.4	10.0 \pm 2.5	17.9 \pm 8.4
16:0	3.6 \pm 0.6	10.7 \pm 1.8	9.1 \pm 1.7	2.3	2.2 \pm 0.5	11.2 \pm 0.9	10.8 \pm 1.6	12.1 \pm 0.5
16:4	4.5 \pm 3.5	1.0 \pm 1.2	0.8 \pm 1.3	0.2	9.8 \pm 0.9	2.0 \pm 1.5	1.5 \pm 1.0	0.3 \pm 0.1
16:1(n-7)	10.6 \pm 0.7	8.9 \pm 1.8	6.9 \pm 3.8	40.0	14.4 \pm 1.7	7.7 \pm 0.7	10.4 \pm 1.4	4.4 \pm 1.0
18:3(n-6)	2.8 \pm 0.6	0.3 \pm 0.2	0.8 \pm 0.5	0.3	1.7 \pm 0.4	1.2 \pm 0.5	1.9 \pm 0.6	1.4 \pm 0.6
18:4	4.2 \pm 2.7	0.6 \pm 0.6	0.9 \pm 0.4	0.0	4.9 \pm 0.5	2.8 \pm 0.5	3.4 \pm 1.3	0.7 \pm 0.3
18:2(n-6)	2.3 \pm 0.4	5.2 \pm 4.4	6.5 \pm 1.1	3.2	5.6 \pm 4.3	2.6 \pm 0.3	3.1 \pm 0.5	3.3 \pm 0.4
18:1(n-9)	3.3 \pm 0.8	8.0 \pm 3.4	8.4 \pm 3.0	34.1	12.9 \pm 1.2	2.2 \pm 0.8	6.6 \pm 2.8	7.0 \pm 0.3
18:1(tr-9)	0.8 \pm 0.3	2.9 \pm 1.6	3.8 \pm 2.0	1.3	2.1 \pm 1.0	2.9 \pm 0.8	2.5 \pm 0.9	4.5 \pm 0.4
20:5(n-3)	17.9 \pm 14.0	16.9 \pm 2.1	12.8 \pm 1.7	4.2	25.3 \pm 3.0	22.1 \pm 1.4	18.4 \pm 2.2	16.8 \pm 3.6
20:1(n-9)	12.5 \pm 2.3	3.1 \pm 1.9	2.6 \pm 0.6	2.0	0.3 \pm 0.1	3.3 \pm 3.8	5.4 \pm 0.9	2.5 \pm 0.6
22:6(n-3)	8.9 \pm 1.6	21.8 \pm 5.8	11.5 \pm 1.7	4.5	5.2 \pm 0.6	18.4 \pm 5.9	9.2 \pm 6.5	14.2 \pm 7.0
22:1(n-9)	1.9 \pm 0.5	2.0 \pm 2.3	0.8 \pm 0.4	0.1	0.0 \pm 0.0	0.9 \pm 0.5	0.9 \pm 0.1	0.7 \pm 0.2
20:4	2.3 \pm 1.2	1.0 \pm 1.0	1.0 \pm 0.2	0.1	1.0 \pm 0.2	0.8 \pm 0.4	3.3 \pm 3.0	1.2 \pm 0.4
22:1(n-11)	6.4 \pm 1.5	2.7 \pm 3.9	1.1 \pm 0.6	0.8	0.1 \pm 0.1	1.5 \pm 2.1	2.0 \pm 0.7	1.2 \pm 0.3

16:1(n-7), 14:0 and 22:6(n-3), in agreement with other studies (Fricke and Oehlenschläger, 1988; Nelson et al., 2001; Mayzaud and Boutoute, 2015). The presence of the calanoid biomarker 20:1(n-9), both in fatty acid and alcohol forms, indicates feeding on *C. acutus* or other calanoid copepods. The $\delta^{15}\text{N}$ and estimated trophic level of the amphipod *T. gaudichaudii* was much lower than expected given the species' known

behaviour as a raptorial predator (Pakhomov and Perissinotto, 1996; Froneman et al., 2000; Watts and Tarling, 2012). However, other studies have also reported relatively low $\delta^{15}\text{N}$ signatures in *T. gaudichaudii*, and together with herbivorous fatty acid biomarkers, suggests that this species is likely more omnivorous than previously thought, especially in juvenile stages (Richoux and Froneman, 2009; Richoux, 2011; Stowasser

Table 7

Fatty alcohol composition (mol% mean \pm standard deviation) of the 8 studied zooplankton taxa sampled at station P3 (P3B + P3C) in the Scotia Sea, focusing on the 8 most abundant fatty alcohols included in the RDA model. The number of replicate samples (n) is indicated for each taxon. Replicate samples of *C. acutus* each contained 5 individuals. Replicate samples of *R. gigas* each contained 2 individuals. All other taxa replicates contained 1 individual per replicate.

	<i>Calanoides acutus</i> n = 6	<i>Chaetognatha</i> n = 7	<i>Euphausia triacantha</i> n = 5	<i>Paraeuchaeta</i> spp. n = 1	<i>Rhincalanus gigas</i> n = 7	<i>Salpa thompsoni</i> n = 2	<i>Themisto gaudichaudii</i> n = 3	<i>Thysanoessa</i> spp. n = 5
ALC-14:0	11.3 \pm 1.0	24.3 \pm 16.3	23.0 \pm 0.9	30.0	35.2 \pm 1.0	5.3 \pm 6.2	8.8 \pm 3.3	1.3 \pm 1.3
ALC-16:0	11.1 \pm 0.6	23.7 \pm 16.7	25.1 \pm 0.7	23.5	37.4 \pm 1.9	6.6 \pm 6.1	9.6 \pm 2.3	1.7 \pm 1.5
ALC-18:0	0.5 \pm 0.3	5.1 \pm 6.2	3.8 \pm 0.3	0.8	8.0 \pm 1.3	1.3 \pm 0.6	0.7 \pm 0.0	0.6 \pm 0.4
ALC-16:1	6.5 \pm 0.8	2.1 \pm 2.1	3.9 \pm 0.3	8.4	8.5 \pm 2.6	2.2 \pm 3.0	4.5 \pm 2.3	0.9 \pm 0.4
ALC-18:1	2.8 \pm 0.9	7.7 \pm 10.8	8.0 \pm 1.7	13.3	7.3 \pm 0.6	3.3 \pm 1.2	2.2 \pm 0.8	36.7 \pm 8.9
ALC-20:1	41.6 \pm 2.4	24.2 \pm 19.8	21.4 \pm 0.9	6.1	0.7 \pm 0.2	58.1 \pm 12.9	39.5 \pm 2.6	39.9 \pm 7.3
ALC-22:1	24.9 \pm 2.2	11.4 \pm 9.0	11.5 \pm 3.5	6.3	0.5 \pm 0.1	12.1 \pm 13.6	32.7 \pm 4.6	17.8 \pm 6.6
ALC-24:1	0.6 \pm 0.3	0.3 \pm 0.2	1.4 \pm 0.8	6.8	0.8 \pm 0.3	10.8 \pm 14.4	1.1 \pm 0.7	0.2 \pm 0.2

et al., 2012). Interestingly, the $\delta^{15}\text{N}$ values of *T. gaudichaudii* increased with corresponding increases in $\delta^{15}\text{N}$ of POM with depth (Figs. 1 and 2), suggesting that this species may be tightly linked to the ambient food supply at the depth of its capture. The increased $\delta^{15}\text{N}$ signatures with depth may reflect differences in the developmental-stage due to vertical ontogenetic partitioning, with younger stages in surface waters and older stages (with heavier $\delta^{15}\text{N}$) at depth, which is commonly observed in pelagic amphipods (Bowman et al., 1982; Blankenship et al., 2006; Lacey et al., 2018).

The $\delta^{15}\text{N}$ signatures of *R. gigas* decreased relative to increasing $\delta^{15}\text{N}$ of POM with depth (Figs. 1 and 2), suggesting that this species may not have been feeding directly on ambient POM at the depth at which they were captured, but in surface waters. *R. gigas* has been observed to undergo shallow diel vertical migration (DVM) (Atkinson et al., 1992a, 1992b; Conroy et al., 2020). However, no pronounced synchronised DVM of zooplankton was observed at the time of the study (Cook et al., 2023), suggesting that *R. gigas* in deep waters may not be feeding in surface waters at night. The negative relationship between $\delta^{15}\text{N}$ signatures of *R. gigas* and POM may be due to the deeper-dwelling individuals being metabolically inactive and therefore not feeding on ambient POM. Deeper-dwelling *R. gigas* collected concurrently with the present study had lower specific respiration rates than animals from shallower depths (Cook et al., 2023), supporting this suggestion. This interpretation is further supported by high, but decreasing, lipid levels from visit P3B to P3C (Table 2), suggesting the use of internal energy reserves (see Section 4.3).

4.3. Physiological ecology of copepod species

Differences in lipid and $\delta^{15}\text{N}$ signatures may reflect important, species-specific aspects of zooplankton life cycles and physiological requirements. The lipid class and fatty acid RDA analyses revealed a separation between *C. acutus*, *R. gigas* and *Paraeuchaeta* spp. and the rest of the zooplankton, with each copepod species forming a distinct cluster (Figs. 6 and 7). The lipid class RDA (Fig. 6) and compositional data (Table 5) demonstrate that fatty alcohols were important for discriminating these copepods from the rest of the species. Fatty alcohols are essential in the production of wax esters (WE), which are a major lipid class in these animals (Hagen et al., 1995; Kattner and Hagen, 1995; Lee et al., 2006). The copepods *C. acutus* and *R. gigas* had higher body lipid content (Table 2) compared to the other species, consistent with the seasonal production of large lipid reserves in polar non-carnivorous calanoid copepods (Graeve et al., 1994). Large lipid reserves are important in the ontogenetic behaviour of diapausing copepods, which

migrate to deeper waters to overwinter and use stored lipids to fuel reproductive processes (sexual maturation, gonad development, and egg production/spawning) (Hagen and Schnack-Schiel, 1996) and regulate buoyancy (Pond, 2012). *C. acutus* has a 1-year life cycle with intense grazing in spring/summer followed by a descent into deep waters where they undergo diapause and become inactive (Marin and Schnack-Schiel, 1993; Marin, 1988). *C. acutus* fatty acids were dominated by the PUFA 20:5(n-3) and the MUFAs 20:1(n-9), 16:1(n-7) and 22:1(n-11), in agreement with our understanding of the importance of long-chained moieties for diapausing species (Hagen and Schnack-Schiel, 1996; Pond and Tarling, 2011; Pond et al., 2012).

R. gigas did not contain the calanoid copepod markers, 20:1(n-9) and 22:1(n-11), but instead was dominated by 20:5(n-3) and short-chained fatty acid and alcohol moieties, in agreement with the understanding that fatty acid biosynthesis in *R. gigas* likely ends with the elongation to 18:0 and conversion to 18:1 (Kattner et al., 1994; Ward et al., 1996). This contrasts with the wax ester composition of *C. acutus*, which is dominated by esters of 20:1(n-9) or 20:5(n-3) acids paired to ALC-20:1 (n-9) (Pond and Tarling, 2011; Pond, 2012). *R. gigas* has been observed to have both 1- and 2- year life cycles, and various levels of diapause, with trophic inactivity, semi-activity and active feeding in winter (Marin and Schnack-Schiel, 1993; Hopkins et al., 1993; Ward et al., 1997; Marin, 1988; Pasternak and Schnack-Schiel, 2001; Tarling et al., 2007). Intraspecific differences in life-strategies are likely related to environmental conditions, with *R. gigas* populations at the southern end of their geographical extent having 2-year life cycles due to slow growth rates and harsher environmental conditions (Ward et al., 1997). Given its large, but decreasing lipid reserves and low $\delta^{15}\text{N}$ values, we suggest *R. gigas*, particularly deeper-dwelling individuals, at the P3 site in the Scotia Sea were metabolically inactive and using internal energy stores – indicative of some form of diapause. This highlights the need to understand how animal physiologies influence lipid and $\delta^{15}\text{N}$ signatures, rather than signatures being a reflection of just ecological and feeding dynamics. If overwinter behaviour was not considered, the low $\delta^{15}\text{N}$ signatures and dominance of diatom fatty acid biomarkers in *R. gigas* could be interpreted as their feeding on fresh diatoms from the surface.

The fate of primary production within the food webs of the epipelagic and upper mesopelagic is a major determinant of subsequent carbon sequestration in deeper waters. The different physiological ecologies elucidated from the lipid and stable isotope data highlight the importance of considering physiology when tracing carbon cycling. Determining the extent to which large herbivorous copepod species such as *R. gigas* and *C. acutus* undergo overwintering and hence do or do not always interact with the spring phytoplankton bloom will influence how

we represent their role in attenuating the flux of sinking POM in the epi- and upper mesopelagic. Similarly, determining where and on what zooplankton are feeding will increase our understanding of how these animals interact with and cycle organic matter. For instance, the preferential feeding on fresh, surface-derived POM rather than re-worked particles may modify the quality and quantity of organic matter leaving the upper mesopelagic.

5. Conclusion

The $\delta^{15}\text{N}$ signatures of particulate organic matter (POM) sampled at the P3 site in the Scotia Sea increased with depth, whereas the $\delta^{15}\text{N}$ signatures of zooplankton species generally did not. This suggests a decoupling between the feeding dynamics of zooplankton and ambient POM throughout the upper mesopelagic (>500m) at this location. We propose that non-carnivorous zooplankton in this region typically prefer to feed on surface-derived POM and not reworked particles found in deeper waters. The diatom fatty acid biomarkers, 16:1(n-7) and 20:5(n-3), were abundant in POM sampled at all depths, supporting the idea that fresh, surface-derived sinking POM was available throughout the epi- and upper mesopelagic, negating the need for migration to surface waters to access this material. *R. gigas* was the only non-carnivorous species not to conform to the consumption of diatom-based material throughout the water column; its $\delta^{15}\text{N}$ signature decreased with depth, suggesting that it was not feeding on ambient POM at their depth of capture. We suggest that the deeper-dwelling *R. gigas* and *C. acutus* were likely in the process of emerging from their overwintering physiology and still using stored energy reserves, as indicated by their large but decreasing lipid reserves between sampling visit P3B and P3C. Fatty acid and alcohol profiles of the non-copepod species were similar and characterised by both herbivorous and carnivorous biomarkers, suggesting generalist feeding strategies, in agreement with their life-strategies of active year-round feeding. *T. gaudichaudii* showed signs of potential vertical ontogenetic partitioning, with juvenile stages being more herbivorous than expected given the predatory nature of this species. Our study highlights the complexity of mesopelagic food webs and the importance of taking into account zooplankton physiology and suggests that the application of broad trophic functional types may lead to an incorrect understanding of ecosystem dynamics.

CRedit authorship contribution statement

Eloïse Linda-Roselyne Savineau: Writing – review & editing, Writing – original draft, Visualization, Methodology, Funding acquisition, Formal analysis, Conceptualization. **Kathryn B. Cook:** Writing – review & editing, Supervision, Investigation, Conceptualization. **Sabena J. Blackbird:** Methodology, Investigation. **Gabriele Stowasser:** Writing – review & editing, Methodology, Investigation. **Konstadinos Kiriakoulakis:** Investigation. **Calum Preece:** Investigation. **Sophie Fielding:** Investigation. **Anna C. Belcher:** Writing – review & editing, Investigation. **George A. Wolff:** Writing – review & editing. **Geraint A. Tarling:** Writing – review & editing, Investigation, Funding acquisition. **Daniel J. Mayor:** Writing – review & editing, Supervision, Investigation, Funding acquisition, Conceptualization.

Declaration of competing interest

The authors declare that they have no known competing financial interests or personal relationships that could have appeared to influence the work reported in this paper.

Data availability

Data will be made available on request.

Acknowledgements

The authors thank the crew of the R.R.S. Discovery and participants of cruise DY086 for help collecting samples. We thank the anonymous reviewers for their insightful comments, constructive feedback and time invested in reviewing our work. This work was supported by the Natural Environmental Research Council (NERC) funded Large Grant, COMICS (NE/M020762/1; NE/M020835/1) and the NERC grant (NE/S007210/1).

Appendix A. Supplementary data

Supplementary data to this article can be found online at <https://doi.org/10.1016/j.dsr.2024.104317>.

References

- Ainsworth, J., Poulton, A.J., Lohan, M.C., Stinchcombe, M.C., Lough, A.J.M., Moore, C. M., 2023. Iron cycling during the decline of a South Georgia diatom bloom. *Deep Sea Res. Part II Top. Stud. Oceanogr.*, 105269.
- Anderson, T.R., Hessen, D.O., Gentleman, W.C., Yool, A., Mayor, D.J., 2022. Quantifying the roles of food intake and stored lipid for growth and development throughout the life cycle of a high-latitude copepod, and consequences for ocean carbon sequestration. *Front. Mar. Sci.* 9.
- Atkinson, A., Ward, P., Williams, R., Poulet, S.A., 1992a. Diel vertical migration and feeding of copepods at an oceanic site near South Georgia. *Mar. Biol.* 113 (4), 583–593.
- Atkinson, A., Ward, P., Williams, R., Poulet, S.A., 1992b. Feeding rates and diel vertical migration of copepods near South Georgia: comparison of shelf and oceanic sites. *Mar. Biol.* 114 (1), 49–56.
- Atkinson, A., Siegel, V., Pakhomov, E., Rothery, P., 2004. Long-term decline in krill stock and increase in salps within the Southern Ocean. *Nature* 432 (7013), 100–103.
- Bell, M.V., Dick, J.R., Anderson, T.R., Pond, D.W., 2007. Application of liposome and stable isotope tracer techniques to study polyunsaturated fatty acid biosynthesis in marine zooplankton. *J. Plankton Res.* 29 (5), 417–422.
- Blankenship, L.E., Yayanos, A.A., Cadien, D.B., Levin, L.A., 2006. Vertical zonation patterns of scavenging amphipods from the Hadal zone of the Tonga and Kermadec Trenches. *Deep Sea Res. Oceanogr. Res. Pap.* 53 (1), 48–61.
- Bowman, T.E., Cohen, A.C., McGuinness, M.M., 1982. Vertical Distribution of *Themisto Gaudichaudii* (Amphipoda: Hyperidea) in Deepwater Dumpsite 106 off the Mouth of Delaware Bay.
- Boyd, P.W., Claustre, H., Levy, M., Siegel, D.A., Weber, T., 2019. Multi-faceted particle pumps drive carbon sequestration in the ocean. *Nature* 568 (7752), 327–335.
- Cabana, G., Rasmussen, J.B., 1996. Comparison of aquatic food chains using nitrogen isotopes. *Proc. Natl. Acad. Sci. USA* 93 (20), 10844–10847.
- Conroy, J.A., Steinberg, D.K., Thibodeau, P.S., Schofield, O., 2020. Zooplankton diel vertical migration during Antarctic summer. *Deep Sea Res. Oceanogr. Res. Pap.* 162, 103324.
- Cook, K.B., Belcher, A., Juez, D.B., Stowasser, G., Fielding, S., Saunders, R.A., Elsafi, M. A., Wolff, G.A., Blackbird, S.J., Tarling, G.A., Mayor, D.J., 2023. Carbon budgets of Scotia Sea mesopelagic zooplankton and micronekton communities during austral spring. *Deep Sea Res. Part II Top. Stud. Oceanogr.*, 105296.
- Dalsgaard, J., John, M.S., Kattner, G., Müller-Navarra, D., Hagen, W., 2003. Fatty acid trophic markers in the pelagic marine environment. *Adv. Mar. Biol.* 46, 225–340.
- de Moura, G.C., de Lucena Barbosa, J.E., Patrício, J., Nery, J.F., Gonçalves, A.M.M., 2016. Seasonal and spatial shifts in copepod diets within tropical estuaries measured by fatty acid profiles. *Ecol. Indic.* 69, 284–294.
- Falk-Petersen, S., Sargent, J.R., Lønne, O.J., Timofeev, S., 1999. Functional biodiversity of lipids in Antarctic zooplankton: *Calanoides acutus*, *Calanus propinquus*, *Thysanoessa macrura* and *Euphausia crystallorophias*. *Polar Biol.* 21 (1), 37–47.
- Fricke, H., Oehlenschläger, J., 1988. Fatty acid and sterol composition of the Antarctic amphipod *Themisto gaudichaudii* Guerin 1828. *Comp. Biochem. Physiol. Part B: Comparative Biochemistry* 89 (1), 39–42.
- Froneman, P.W., Pakhomov, E.A., 1998. Trophic importance of the chaetognaths *Eukrohnia hamata* and *Sagitta gazellae* in the pelagic system of the Prince Edward Islands (Southern Ocean). *Polar Biol.* 19 (4), 242–249.
- Froneman, P.W., Pakhomov, E.A., Perissinotto, R., Meaton, V., 1998. Feeding and predation impact of two chaetognath species, *Eukrohnia hamata* and *Sagitta gazellae*, in the vicinity of Marion Island (southern ocean). *Mar. Biol.* 131 (1), 95–101.
- Froneman, P.W., Pakhomov, E.A., Treasure, A., 2000. Trophic importance of the hyperiid amphipod *Themisto gaudichaudii*, in the Prince Edward Archipelago (Southern Ocean) ecosystem. *Polar Biol.* 23 (6), 429–436.
- Giering, S.L., Sanders, R., Lampitt, R.S., Anderson, T.R., Tamburini, C., Boutrif, M., Zubkov, M.V., Marsay, C.M., Henson, S.A., Saw, K., Cook, K., 2014. Reconciliation of the carbon budget in the ocean's twilight zone. *Nature* 507 (7493), 480–483.
- Giering, S.L.C., Sanders, R.J., Stinchcombe, M., Henson, S.A., Carvalho, F., Lampitt, R.S., Iversen, M., Kiriakoulakis, K., Moore, M.C., Ainsworth, J., Poulton, A.J., Evans, C., Lam, P., Fuessel, J., Rayne, R., Hemsley, V., Laurenceau-Cornec, E., Mayor, D.J., Cook, K.B., Tarling, G.A., Fielding, S., Stowasser, G., Belcher, A., Saw, K., Ashurst, D., Shepard, O., Bridger, M., Wynar, J., Rundle, N., Roberts, T., 2019. RRS Discovery cruise DY086, 12 November – 19 December 2017. Controls over Ocean Mesopelagic

- Carbon Storage (COMICS). National Oceanography Centre Cruise Report. No. 55, 265pp.
- Giering, S.L.C., Sanders, R., Blackbird, S., Briggs, N., Carvalho, F., East, H., Espinola, B., Henson, S.A., Kiriakoulakis, K., Iversen, M.H., Lampitt, R.S., 2023. Vertical imbalance in organic carbon budgets is indicative of a missing vertical transfer during a phytoplankton bloom near South Georgia (COMICS). *Deep Sea Res. Part II Top. Stud. Oceanogr.* 209, 105277.
- Graeve, M., Hagen, W., Kattner, G., 1994. Herbivorous or omnivorous? On the significance of lipid compositions as trophic markers in Antarctic copepods. *Deep Sea Res. Oceanogr. Res. Pap.* 41 (5–6), 915–924.
- Hagen, W., Kattner, G., Graeve, M., 1993. *Calanoides acutus* and *Calanus propinquus*, Antarctic copepods with different lipid storage modes via wax esters or triacylglycerols. *Mar. Ecol. Prog. Ser.* 135–142.
- Hagen, W., Kattner, G., Graeve, M., 1995. On the lipid biochemistry of polar copepods: compositional differences in the Antarctic calanoids *Euchaeta antarctica* and *Euchirella rostromagna*. *Mar. Biol.* 123 (3), 451–457.
- Hagen, W., Schnack-Schiel, S.B., 1996. Seasonal lipid dynamics in dominant Antarctic copepods: energy for overwintering or reproduction? *Deep Sea Res. Oceanogr. Res. Pap.* 43 (2), 139–158.
- Hopkins, T.L., 1985. Food web of an Antarctic midwater ecosystem. *Mar. Biol.* 89 (2), 197–212.
- Hopkins, T.L., Lancraft, T.M., Torres, J.J., Donnelly, J., 1993. Community structure and trophic ecology of zooplankton in the Scotia Sea marginal ice zone in winter (1988). *Deep Sea Res. Oceanogr. Res. Pap.* 40 (1), 81–105.
- Ikeda, T., 1988. Metabolism and chemical composition of crustaceans from the Antarctic mesopelagic zone. *Deep-Sea Res., Part A* 35 (12), 1991–2002.
- Kates, M., Volcani, B.E., 1966. Lipid components of diatoms. *Biochim. Biophys. Acta Lipids Lipid. Metabol.* 116 (2), 264–278.
- Kattner, G., Graeve, M., Hagen, W., 1994. Ontogenetic and seasonal changes in lipid and fatty acid/alcohol compositions of the dominant Antarctic copepods *Calanus propinquus*, *Calanoides acutus* and *Rhincalanus gigas*. *Mar. Biol.* 118 (4), 637–644.
- Kattner, G., Hagen, W., 1995. Polar herbivorous copepods—different pathways in lipid biosynthesis. *ICES (Int. Counc. Explor. Sea) J. Mar. Sci.* 52 (3–4), 329–335.
- Kattner, G., Albers, C., Graeve, M., Schnack-Schiel, S.B., 2003. Fatty acid and alcohol composition of the small polar copepods, *Oithona* and *Oncaea*: indication on feeding modes. *Polar Biol.* 26 (10), 666–671.
- Kiriakoulakis, K., Bett, B.J., White, M., Wolff, G.A., 2004. Organic biogeochemistry of the Darwin Mounds, a deep-water coral ecosystem, of the NE Atlantic. *Deep Sea Res. Oceanogr. Res. Pap.* 51 (12), 1937–1954.
- Korb, R.E., Whitehouse, M.J., Ward, P., Gordon, M., Venables, H.J., Poulton, A.J., 2012. Regional and seasonal differences in microplankton biomass, productivity, and structure across the Scotia Sea: implications for the export of biogenic carbon. *Deep Sea Res. Part II Top. Stud. Oceanogr.* 59, 67–77.
- Koski, M., Valencia, B., Newstead, R., Thiele, C., 2020. The missing piece of the upper mesopelagic carbon budget? Biomass, vertical distribution and feeding of aggregate-associated copepods at the PAP site. *Prog. Oceanogr.* 181, 102243.
- Kruse, S., Hagen, W., Bathmann, U., 2010. Feeding ecology and energetics of the Antarctic chaetognaths *Eukrohnia hamata*, *E. bathypelagica* and *E. bathyantartica*. *Mar. Biol.* 157 (10), 2289–2302.
- Kwon, E.Y., Primeau, F., Sarmiento, J.L., 2009. The impact of remineralization depth on the air-sea carbon balance. *Nat. Geosci.* 2, 630–635.
- Lacey, N.C., Mayor, D.J., Linley, T.D., Jamieson, A.J., 2018. Population structure of the hadal amphipod *Bathycallistoma (Scopelocheirus) schellenbergi* in the Kermadec trench and New Hebrides trench, SW Pacific. *Deep Sea Res. Part II Top. Stud. Oceanogr.* 155, 50–60.
- Lee, R.F., Hagen, W., Kattner, G., 2006. Lipid storage in marine zooplankton. *Mar. Ecol. Prog. Ser.* 307, 273–306.
- Manno, C., Stowasser, G., Fielding, S., Apeland, B., Tarling, G.A., 2022. Deep carbon export peaks are driven by different biological pathways during the extended Scotia Sea (Southern Ocean) bloom. *Deep Sea Res. Part II Top. Stud. Oceanogr.* 205, 105183.
- Marin, V., 1988. Qualitative models of the life cycles of *Calanoides acutus*, *Calanus propinquus*, and *Rhincalanus gigas*. *Polar Biol.* 8 (6), 439–446.
- Marin, V.H., Schnack-Schiel, S.B., 1993. The occurrence of *Rhincalanus gigas*, *Calanoides acutus*, and *Calanus propinquus* (Copepoda: Calanoida) in late may in the area of the Antarctic Peninsula. *Polar Biol.* 13 (1), 35–40.
- Mayor, D.J., Cook, K., Thornton, B., Walsham, P., Witte, U.F., Zuur, A.F., Anderson, T.R., 2011. Absorption efficiencies and basal turnover of C, N and fatty acids in a marine Calanoid copepod. *Funct. Ecol.* 25 (3), 509–518.
- Mayor, D.J., Sharples, C.J., Webster, L., Walsham, P., Lacaze, J.P., Cousins, N.J., 2013. Tissue and size-related changes in the fatty acid and stable isotope signatures of the deep sea grenadier fish *Coryphaenoides armatus* from the Charlie-Gibbs Fracture Zone region of the Mid-Atlantic Ridge. *Deep Sea Res. Part II Top. Stud. Oceanogr.* 98, 421–430.
- Mayor, D.J., Sanders, R., Giering, S.L., Anderson, T.R., 2014. Microbial gardening in the ocean's twilight zone: detritivorous metazoans benefit from fragmenting, rather than ingesting, sinking detritus: fragmentation of refractory detritus by zooplankton beneath the euphotic zone stimulates the harvestable production of labile and nutritious microbial biomass. *Bioessays* 36 (12), 1132–1137.
- Mayor, D.J., Gentleman, W.C., Anderson, T.R., 2020. Ocean carbon sequestration: particle fragmentation by copepods as a significant unrecognized factor? Explicitly representing the role of copepods in biogeochemical models may fundamentally improve understanding of future ocean carbon storage. *Bioessays* 42 (12), 2000149.
- Mayzaud, P., Boutoute, M., 2015. Dynamics of lipid and fatty acid composition of the hyperiid amphipod *Themisto*: a bipolar comparison with special emphasis on seasonality. *Polar Biol.* 38 (7), 1049–1065.
- Metfies, K., Nicolaus, A., Von Harbou, L., Bathmann, U., Peeken, I., 2014. Molecular analyses of gut contents: elucidating the feeding of co-occurring salps in the Lazarev Sea from a different perspective. *Antarct. Sci.* 26 (5), 545–553.
- Miyake, Y., Wada, E., 1967. The abundance ratio of ¹⁵N/¹⁴N in marine environments. *Rec. Oceanogr. Works Jpn.* 9, 37–53.
- Nelson, M.M., Mooney, B.D., Nichols, P.D., Phleger, C.F., 2001. Lipids of Antarctic Ocean amphipods: food chain interactions and the occurrence of novel biomarkers. *Mar. Chem.* 73 (1), 53–64.
- Oksanen, J., Blanchet, F.G., Friendly, M., Kindt, R., Legendre, P., McGlenn, D., Minchin, P., O'Hara, R.B., Simpson, G., Solymos, P., Stevens, M.H.H., 2020. Vegan: community ecology package. R package version 2, 5–7 November 2020.
- Øresland, V., 1991. Feeding of the carnivorous copepod *Euchaeta antarctica* in Antarctic waters. *Mar. Ecol. Prog. Ser.* 78, 41–47.
- Øresland, V., Ward, P., 1993. Summer and winter diet of four carnivorous copepod species around South Georgia. *Mar. Ecol. Prog. Ser.* 73–78.
- Pakhomov, E.A., Perissinotto, R., 1996. Trophodynamics of the hyperiid amphipod *Themisto gaudichaudi* in the South Georgia region during late austral summer. *Mar. Ecol. Prog. Ser.* 134, 91–100.
- Pakhomov, E.A., Perissinotto, R., Froneman, P.W., 1999. Predation impact of carnivorous macrozooplankton and micronekton in the Atlantic sector of the Southern Ocean. *J. Mar. Syst.* 19 (1–3), 47–64.
- Pakhomov, E.A., Henschke, N., Hunt, B.P., Stowasser, G., Cherel, Y., 2019. Utility of salps as a baseline proxy for food web studies. *J. Plankton Res.* 41 (1), 3–11.
- Pasternak, A.F., Schnack-Schiel, S.B., 2001. Feeding patterns of dominant Antarctic copepods: an interplay of diapause, selectivity, and availability of food. *Hydrobiologia* 453 (1), 25–36.
- Phleger, C.F., Nichols, P.D., Virtue, P., 1998. Lipids and trophodynamics of Antarctic zooplankton. *Comp. Biochem. Physiol. B Biochem. Mol. Biol.* 120 (2), 311–323.
- Pond, D.W., Tarling, G.A., 2011. Phase transitions of wax esters adjust buoyancy in diapausing *Calanoides acutus*. *Limnol. Oceanogr.* 56 (4), 1310–1318.
- Pond, D.W., 2012. The physical properties of lipids and their role in controlling the distribution of zooplankton in the oceans. *J. Plankton Res.* 34 (6), 443–453.
- Pond, D.W., Tarling, G.A., Ward, P., Mayor, D.J., 2012. Wax ester composition influences the diapause patterns in the copepod *Calanoides acutus*. *Deep Sea Res. Part II Top. Stud. Oceanogr.* 59, 93–104.
- Pond, D.W., Tarling, G.A., Mayor, D.J., 2014. Hydrostatic pressure and temperature effects on the membranes of a seasonally migrating marine copepod. *PLoS One* 9 (10).
- Post, D.M., 2002. Using stable isotopes to estimate trophic position: models, methods, and assumptions. *Ecology* 83 (3), 703–718.
- Preece, C., Blackbird, S., Kiriakoulakis, K., Cook, K., Mayor, D.J., Savineau, E.L.-R., Giering, S., Stowasser, G., Tarling, G., Wolff, G.A., Submitted. Particulate Organic Matter and the Influence of Zooplankton on its Composition and Fate in the Mesopelagic Zone, Scotia Sea, (Southern Ocean).
- Protopapa, M., Koppelman, R., Zervoudaki, S., Wunsch, C., Peters, J., Parinos, C., Paraschos, F., Gogou, A., Möllmann, C., 2019. Trophic positioning of prominent copepods in the epi-and mesopelagic zone of the ultra-oligotrophic eastern Mediterranean Sea. *Deep Sea Res. Part II Top. Stud. Oceanogr.* 164, 144–155.
- Richoux, N.B., Froneman, P.W., 2009. Plankton trophodynamics at the subtropical convergence, Southern Ocean. *J. Plankton Res.* 31 (9), 1059–1073.
- R Core Team, 2022. R: A Language and Environment for Statistical Computing. R Foundation for Statistical Computing, Vienna, Austria.
- Richoux, N.B., 2011. Trophic ecology of zooplankton at a frontal transition zone: fatty acid signatures at the subtropical convergence, Southern Ocean. *J. Plankton Res.* 33 (3), 491–505.
- Sanders, R.J., Henson, S.A., Martin, A.P., Anderson, T.R., Bernardello, R., Enderlein, P., Fielding, S., Giering, S.L., Hartmann, M., Iversen, M., Khatiwala, S., Lam, P., Lampitt, R., Mayor, D.J., Moore, M.C., Murphy, E., Painter, S.C., Poulton, A.J., Saw, K., Stowasser, G., Tarling, G.A., Torres-Valdes, S., Trimmer, M., Wolff, G.A., Yool, A., Zubkov, M., 2016. Controls over ocean mesopelagic interior carbon storage (COMICS): fieldwork, synthesis, and modeling efforts. *Front. Mar. Sci.* 3, 136.
- Sheridan, C.C., Lee, C., Wakeham, S.G., Bishop, J.K.B., 2002. Suspended particle organic composition and cycling in surface and midwaters of the equatorial Pacific Ocean. *Deep Sea Res. Oceanogr. Res. Pap.* 49 (11), 1983–2008.
- Søreide, J.E., Falk-Petersen, S., Hegseth, E.N., Hop, H., Carroll, M.L., Hobson, K.A., Blachowiak-Samolyk, K., 2008. Seasonal feeding strategies of *Calanus* in the high-Arctic Svalbard region. *Deep Sea Res. Part II Top. Stud. Oceanogr.* 55 (20–21), 2225–2244.
- Steinberg, D.K., Landry, M.R., 2017. Zooplankton and the ocean carbon cycle. *Ann. Rev. Mar. Sci.* 9 (1), 413–444.
- Stevens, C.J., Sahota, R., Galbraith, M.D., Venello, T.A., Bazinet, A.C., Hennekes, M., Yongblat, K., Juniper, S.K., 2022. Total lipid and fatty acid composition of mesozooplankton functional group members in the NE Pacific over a range of productivity regimes. *Mar. Ecol. Prog. Ser.* 687, 43–64.
- Stowasser, G., Atkinson, A., McGill, R.A.R., Phillips, R.A., Collins, M.A., Pond, D.W., 2012. Food web dynamics in the Scotia Sea in summer: a stable isotope study. *Deep Sea Res. Part II Top. Stud. Oceanogr.* 59, 208–221.
- Tarling, G.A., Shreeve, R.S., Ward, P., 2007. Life-cycle and population dynamics of *Rhincalanus gigas* (Copepoda: Calanoida) in the Scotia Sea. *Mar. Ecol. Prog. Ser.* 338, 145–158.
- Turner, J.T., 2015. Zooplankton fecal pellets, marine snow, phytodetritus and the ocean's biological pump. *Prog. Oceanogr.* 130, 205–248.
- Vander Zanden, M.J., Rasmussen, J.B., 2001. Variation in $\delta^{15}\text{N}$ and $\delta^{13}\text{C}$ trophic fractionation: implications for aquatic food web studies. *Limnol. Oceanogr.* 46 (8), 2061–2066.

- Ventura, M., 2006. Linking biochemical and elemental composition in freshwater and marine crustacean zooplankton. *Mar. Ecol. Prog. Ser.* 327, 233–246.
- Visser, A.W., Jónasdóttir, S.H., 1999. Lipids, buoyancy and the seasonal vertical migration of *Calanus finmarchicus*. *Fish. Oceanogr.* 8, 100–106.
- von Harbou, L., Dubischar, C.D., Pakhomov, E.A., Hunt, B.P., Hagen, W., Bathmann, U. V., 2011. Salps in the Lazarev sea, Southern Ocean: I. Feeding dynamics. *Mar. Biol.* 158, 2009–2026.
- Ward, P., Shreeve, R.S., Cripps, G.C., 1996. *Rhincalanus gigas* and *Calanus simillimus*: lipid storage patterns of two species of copepod in the seasonally ice-free zone of the Southern Ocean. *J. Plankton Res.* 18 (8), 1439–1454.
- Ward, P., Atkinson, A., Schnack-Schiel, S.B., Murray, A.W.A., 1997. Regional variation in the life cycle of *Rhincalanus gigas* (Copepoda: Calanoida) in the Atlantic sector of the Southern Ocean—re-examination of existing data (1928 to 1993). *Mar. Ecol. Prog. Ser.* 157, 261–275.
- Ward, P., Atkinson, A., Tarling, G., 2012. Mesozooplankton community structure and variability in the Scotia Sea: a seasonal comparison. *Deep Sea Res. Part II Top. Stud. Oceanogr.* 59, 78–92.
- Watts, J., Tarling, G.A., 2012. Population dynamics and production of *Themisto gaudichaudii* (Amphipoda, hyperiidae) at South Georgia, Antarctica. *Deep Sea Res. Part II Top. Stud. Oceanogr.* 59, 117–129.
- Wilson, S.E., Steinberg, D.K., Chu, F.L., Bishop, J.K.B., 2010. Feeding ecology of mesopelagic zooplankton of the subtropical and subarctic North Pacific Ocean determined with fatty acid biomarkers. *Deep Sea Res. Oceanogr. Res. Pap.* 57 (10), 1278–1294.
- Zuur, A.F., Ieno, E.N., Smith, G.M., 2007. Principal Component Analysis and Redundancy Analysis, pp. 193–224. *Analysing ecological data*.